

Self-Assembly of Dithiolene-based Coordination Polymers of Mercury(II): Dithioether *versus* Thiocarbonyl Bonding[#]

Aurélien Hameau¹, Fabrice Guyon¹, Michael Knorr^{1,*},
Mironel Enescu², and Carsten Strohmann³

¹ Laboratoire de Chimie des Matériaux et Interfaces, Faculté des Sciences et Techniques, University of Franche-Comté, 25030 Besançon, France

² Laboratoire de Microanalyses Nucléaires, UMR CEA E4, Faculté des Sciences et Techniques, University of Franche-Comté

³ Institut für Anorganische Chemie der Universität Würzburg, D-97074 Würzburg, Germany

Received December 19, 2005; accepted January 25, 2006

Published online May 3, 2006 © Springer-Verlag 2006

Summary. The reactions of 4,5-bis(methylthio)-1,3-dithiole-2-thione (*L*) with mercury(II) halides allowed the isolation and structural characterization of three novel coordination polymers, $[\text{HgX}_2\text{L}]_n$ ($X = \text{I}$, **1**; $X = \text{Br}$, **2**; $X = \text{Cl}$, **3**). In all cases, the complexation of *L* on HgX_2 occurs *via* the thiocarbonyl function. The strength of this Hg–S bond decreases from $X = \text{I}$ to $X = \text{Cl}$, as indicated by the increasing Hg–S bond distances (2.583(4) **1**; 2.668(4) **2**; 2.815(5) Å **3**). The 1D polymeric structures result from bridging halide interactions and a combination of π – π and S··S interactions between the sulfur rich ligands. The coordination around the Hg center is distorted tetrahedral in **1**, whereas the geometry around the mercury in **3** is better described as distorted square pyramidal. In addition, weak interchain interactions are observed in the crystalline state. The preference of HgI_2 for thiocarbonyl bonding instead of a chelating dithioether bonding was also studied by means of *ab initio* calculations.

Keywords. Inorganic polymers; 1,3-Dithiole-2-thione; X-Ray structure determination; *Ab initio* calculations; Molecular wire.

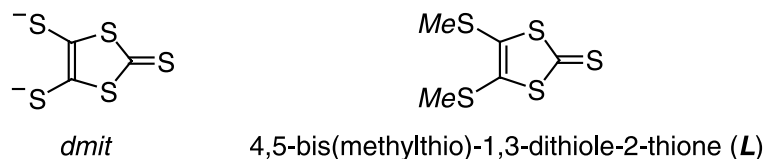
Introduction

Sulfur-rich dithiolenes derived from the tetrathiafulvalene (*TTF*), such as 1,3-dithiole-2-thione-4,5-dithiolate (*dmit*), have been extensively used for the elaboration of conducting or superconducting materials [1]. The importance of these ligands for the design of synthetic metals is largely due to their ability to overlap with each other and to create a network of intermolecular interactions, a prerequisite

* Corresponding author. E-mail: michael.knorr@univ-fcomte.fr

[#] Dedicated to Prof. Dr. Ulrich Schubert on the occasion of his 60th anniversary

for collective electronic properties such as conductivity. Coordination chemistry of thioether compounds derived from this class of dithiolenes has received significant attention only since 10 years in the context of supramolecular chemistry [2]. An important aspect in this domain is the design and the construction of networks of coordination polymers *via* self-assembly through non-covalent interactions. Besides their structural diversity and fascinating topologies, their potential applications as functional materials promote research in this field [3]. In the context of our work on coordination chemistry of multidentate thioether ligands [4] and our experience in dithiolenes chemistry [5], we set out to evaluate the coordinative properties of the 4,5-bis(methylthio)-1,3-dithiole-2-thione (**L**) towards mercury halides HgX_2 .



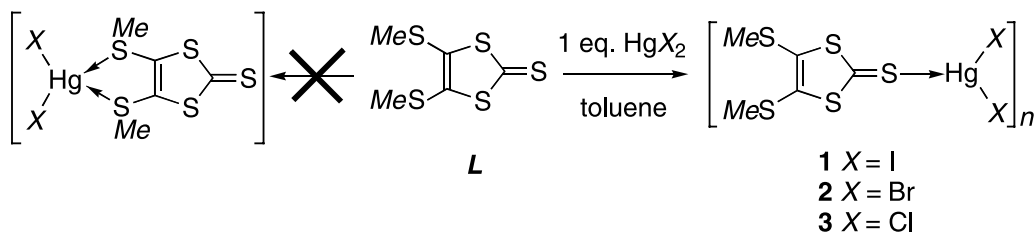
Predicting the result of a self-assembly process is still not easy, as it depends on minute changes of a wide variety of factors. For example, *Munakata et al.* have shown that copper(I) halides react with tetrakis(methylthio)tetrathiafulvalene (*TMT-TTF*) to give coordination polymers, in which the copper halogen frameworks are strongly influenced by the nature of the halogen [2a]. We have recently shown that coordination polymers containing HgX_2 can be built up using thioether ligands such as 1,4-bis(phenylthio)butane [4a] or the tetradentate silane $\text{Si}(\text{CH}_2\text{SR})_4$ [4c]. In continuation of this work, we were interested in the study of the coordination mode of **L** on HgX_2 . This system may act *a priori* as a chelating ligand through the two methylthioether groups or as a *quasi*-monodentate ligand through the exocyclic sulfur atom according to the results obtained with the *TMT-TTF* [2i] and the 4,5-ethylenedithio-1,3-dithiole-2-thione ligands [2c].

In this paper, we report on the synthesis and structural characterization of the compounds obtained by self-assembly between **L** and mercury halides HgX_2 ($X = \text{Cl}, \text{Br}, \text{I}$). To account for the coordination mode of **L** (chelating dithioether or thiocarbonyl), we also investigate the bonding interactions by means of MP2 calculations.

Results and Discussions

Synthesis of $[\{\text{Me}_2\text{dmit}\}\text{HgX}_2]_n$

L reacts in hot toluene with one equivalent of mercury(II) halide to afford the corresponding compounds $[\text{HgX}_2\text{L}]_n$ ($X = \text{I}$, **1**; $X = \text{Br}$, **2**; $X = \text{Cl}$, **3**), isolated as air-stable crystalline solids in 65–75% yield according to Scheme 1. The $\text{C}=\text{S}$ vibration of the ligand **L** in the IR spectra of **2** and **3** appears at the same frequency as the one of the free ligand (1057 cm^{-1}). In contrast, this vibration is shifted to lower wavenumbers in the case of complex **1** (1019 cm^{-1}). This observation indicates a complexation of **L** on HgI_2 *via* the thiocarbonyl function rather than *via*



Scheme 1

the two methylthioether groups. Moreover, we failed to isolate an dithioether adduct from HgI_2 and the **L** analogue carbonyl ligand, *i.e.* the 4,5-bis(methylthio)-1,3-dithiole-2-one. This finding contrasts with previous literature reports on the coordination of HgI_2 by aliphatic dithioether ligands [2i]. These observations indicate the low ability of **L** to act as chelating bidentate ligand *via* the two thioether groups. The exclusive thiocarbonyl coordination of **L** and the polymeric nature of the three compounds **1–3** were finally ascertained by crystal structure determinations. Their solid-state arrangements present some common features, which are however significantly affected by the nature of the mercury halide. Therefore, the crystal structure of **1** will be first presented in detail and then the influence of the halide on the pertinent structural parameters of derivatives **2** and **3** will be discussed.

Crystal Structure of **1**

The crystal structure of **1** exhibits a one-dimensional propagation of the monomeric $[\text{HgI}_2\text{L}]$ motif along the *b* direction, constructed by bridging iodo ligands (Fig. 1).

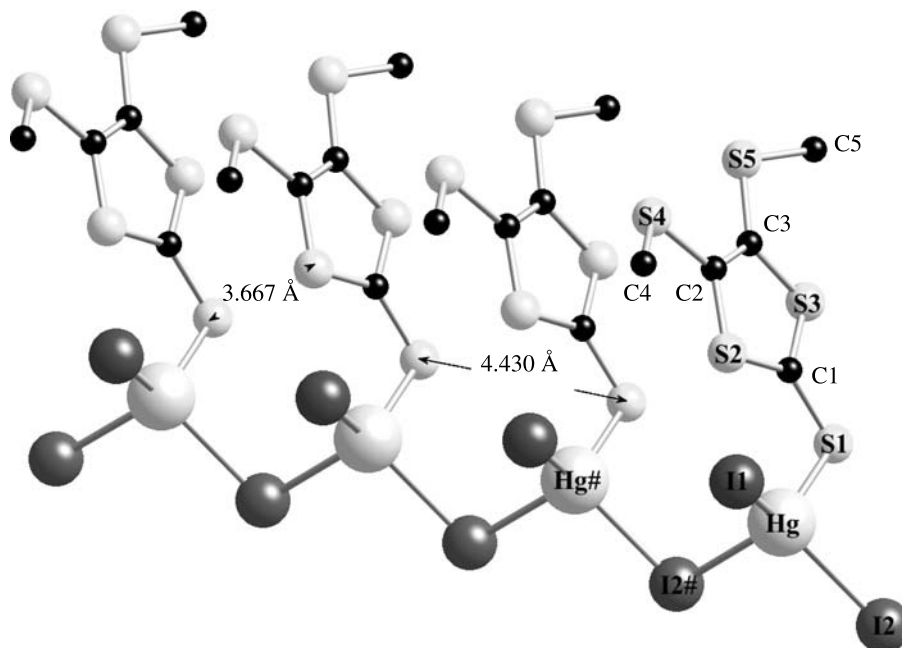


Fig. 1. View of the crystal structure of $[\text{HgI}_2\text{L}]_n$ (**1**) along the *b* axis

Table 1. Selected bond lengths [Å] and angles [°] for **1**, **2**, and **3**

Compound	1 (X = I)	2 (X = Br)	3 (X = Cl)
C(1)–S(1)	1.683(16)	1.693(12)	1.635(18)
C(1)–S(2)	1.737(17)	1.689(13)	1.713(17)
C(1)–S(3)	1.729(18)	1.720(15)	1.764(18)
C(2)–C(3)	1.37(3)	1.34(2)	1.33(2)
C(2)–S(2)	1.719(19)	1.737(13)	1.742(19)
C(2)–S(4)	1.794(18)	1.756(13)	1.772(19)
C(3)–S(3)	1.744(17)	1.744(13)	1.757(17)
C(3)–S(5)	1.749(19)	1.753(15)	1.772(18)
C(4)–S(4)	1.82(3)	1.78(2)	1.79(2)
C(5)–S(5)	1.80(2)	1.765(18)	1.836(17)
X(1)–Hg	2.6822(14)	2.4851(15)	2.399(4)
X(2)–Hg	2.8445(13)	2.4932(14)	2.376(4)
Hg–X(2)#	2.9273(14)	3.0864(15)	3.060
Hg–S(1)	2.583(4)	2.668(4)	2.815(5)
S(1)–C(1)–S(2)	125.2(10)	125.9(9)	126.3(11)
S(1)–C(1)–S(3)	121.4(10)	120.2(8)	122.2(10)
S(2)–C(1)–S(3)	113.3(9)	113.9(7)	111.6(10)
C(3)–C(2)–S(4)	121.4(14)	122.1(10)	122.3(14)
S(2)–C(2)–S(4)	121.1(11)	119.9(8)	120.4(10)
C(2)–C(3)–S(3)	115.0(14)	114.2(10)	115.1(14)
X(1)–Hg–X(2)	117.56(5)	149.86(7)	165.56(16)
X(2)–Hg–X(2)#	100.24(4)	94.96(5)	93.55(2)
X(2)–Hg–S(1)	97.62(10)	106.59(9)	94.15(15)
S(1)–Hg–X(2)#	96.48(10)	98.39(10)	103.56(7)
X(1)–Hg–X(2)#	114.23(5)	89.03(5)	85.57(5)
X(1)–Hg–S(1)	125.96(9)	102.33(9)	100.08(14)
C(1)–S(1)–Hg	104.7(6)	107.0(5)	107.4(6)
C(2)–S(4)–C(4)	101.2(9)	102.4(8)	103.4(9)
C(3)–S(5)–C(5)	103.9(9)	103.0(8)	102.1(8)

Each Hg atom coordinates with three iodine atoms and the sulfur of the thiocarbonyl function of **L**. These atoms are arranged in a distorted tetrahedral manner, the angles being in the range 97.62(10)–125.96(9)° (Table 1). The bridging I(2) ligands are not far from a symmetrical bridging mode between two mercury atoms (2.8445(13) and 2.9273(14) Å). The distance between Hg and the terminal I(1) atom (2.6822(14) Å) is significantly longer than the Hg–I distance in the gaseous phase of HgI₂ (2.57 Å) [6].

The Hg–S(1) bond distance of 2.583(4) Å is similar to the one reported for 4,5-(phenylethylenedithio)-1,3-dithiole-2-thione ligated on HgI₂ (2.567 Å) [7] and much shorter than the Hg–S(thioether) bonds of the complex [(TMT-TTF)(HgI₂)₂] (3.038(2) and 3.157(3) Å) [2i]. The C=S bond is only weakly affected by coordination of the sulfur atom on Hg(II) (1.683(16) Å vs. 1.647(3) Å in free **L** [8]).

The ligands **L**, in which the 1,3-dithiole-2-thione skeleton and the two C atoms of the thiomethyl groups are almost coplanar, adopt a parallel orientation along the *b* axis. The plane to plane separation (with planes defined by the C₃S₂ rings)

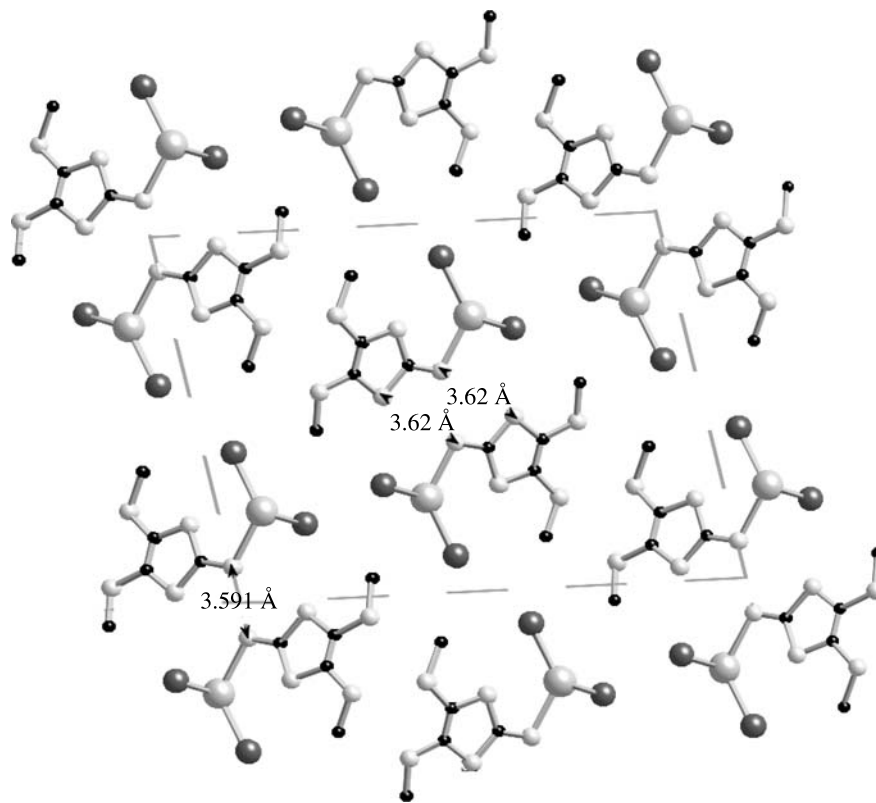


Fig. 2. Projection of the unit-cell content of **1** onto the (a, c) plane showing the inter-ribbons $S \cdots S$ interactions

amounts to 3.70 \AA , the shortest intra-ribbon $S \cdots S$ contacts being 3.668 \AA , somewhat inferior to the sum of the *van der Waals* radii of two S atoms. This difference is due to a slight deviation from ideal planarity between the thiocarbonyl and the five-membered C_3S_2 cycle. Thus, in addition to the bridging iodide interactions, the combination of $\pi-\pi$ and $S \cdots S$ interactions confers a supplementary stabilization to the molecular rod. The bonding situation is best compared with that recently reported by *Dai et al.* for the polymeric compound $[CuIL]_n$ displaying a ladder-like ribbon [2e]. In the latter compound, the shortest intra-ribbon contact is 3.578 \AA . The wire-like assemblies found for **1** are furthermore connected *via* inter-chains $S \cdots S$ contacts, the shortest being 3.591 \AA . In the resulting centrosymmetrical dimers, a head to tail organization is observed (Fig. 2). Note that for the above mentioned $[CuIL]_n$ polymer, substantially closer $S \cdots S$ interactions of 3.268 \AA have been reported [2e].

Crystal Structures of 2 and 3

The nature of the halide in $[HgX_2L]_n$ has no influence on the bonding mode between HgX_2 and **L**. However, a drastically diminution of the bond strengths between these entities is observed from $X = I$ to $X = Cl$ as pointed out by the IR spectroscopic data. The bond between the sulfur of the thiocarbonyl group of **L** and the HgX_2 unit is weakened when the electronegativity of the halide increases, as evidenced by the

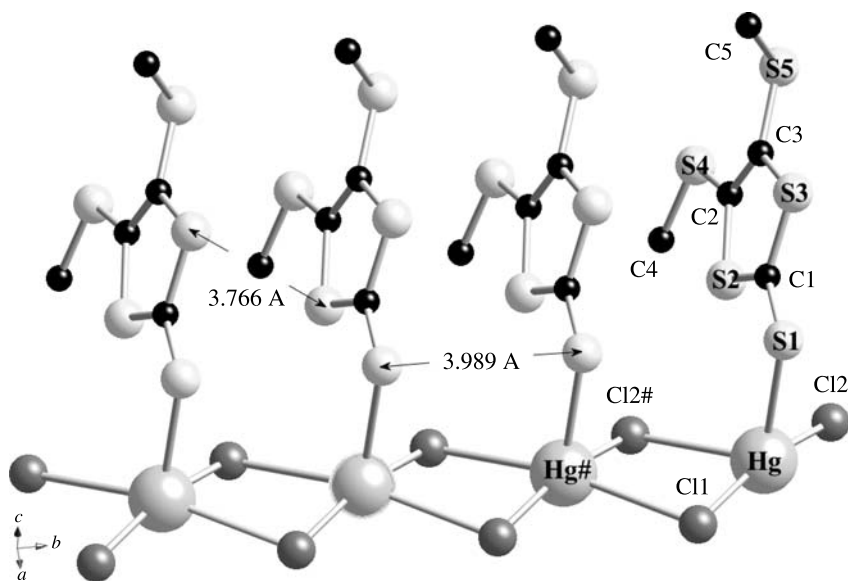


Fig. 3. View of the crystal structure of $[\text{HgCl}_2\text{L}]_n$ (**3**) along the b axis

increasing Hg–S distance (Hg–S = 2.583(4) **1**; 2.668(4) **2**; 2.815(5) Å **3**). Notably, the Hg–S distance in **3** is significantly longer than the one reported upon coordination of 4,5-ethylenedithio-1,3-dithiole-2-thione (2.467(2) Å) [2c], 4,5-diphenylethylenedithio-1,3-dithiole-2-thione (2.392(4) Å) [2h], and the ω -thiocaprolactam (2.496(2) Å) on HgCl_2 [9]. The one-dimensional ribbon in **3** results from the bonding of the HgCl_2 units through two chlorine bridges, thus giving rise to centrosymmetric four-membered $\text{Hg}(\mu\text{-Cl})_2\text{Hg}$ motif (Fig. 3).

The quite long Hg–Cl(2)# and Hg–Cl(1)# bond distances (3.06 and 3.08 Å, respectively) compared to those of Hg–Cl(2) and Hg–Cl(1) (2.376 and 2.399 Å, respectively) indicate the weak bridging contribution of both chlorines. A chlorine atom of another chain is located approximately in *trans* position relative to the S(1) atom (Fig. 4), but the $\text{Hg}\cdots\text{Cl}$ separation of 3.40 Å falls in the limit of *van der Waals* interactions (3.50 Å). Therefore, the coordination environment around the mercury centers is best described as distorted square pyramidal with *trans* Cl–Hg–Cl angles of 165.56 and 168.76°, the mercury atom being at 0.30 Å out of the plane defined by the chlorine atoms (Fig. 3). The $\text{Hg}\cdots\text{Hg}\#$ separation of 3.988 Å in **3** is much shorter than that observed for **1** (4.43 Å), but excludes any bonding interaction between the two d^{10} centers.

In the case of the bromo derivative **2**, the coordination mode around the mercury atoms is intermediate between the situations encountered for **1** and **3** (see Fig. 4 and Table 1).

Again, the quasi-planar 1,3-dithiole-2-thione cores adopt a parallel orientation in the chains of **2** and **3**, with plane to plane distances of 3.66 and 3.58 Å. Although these separations are shorter than the one found for **1**, the shortest S \cdots S interactions are not strengthened (3.761 Å for **3** and 3.924 Å for **2**) due to the relative orientation of the ligands, which does not optimize the overlap. In contrast to **1**, only one thiomethyl group is coplanar to the C_3S_5 cycle of **2** and **3**, the second one being significantly out

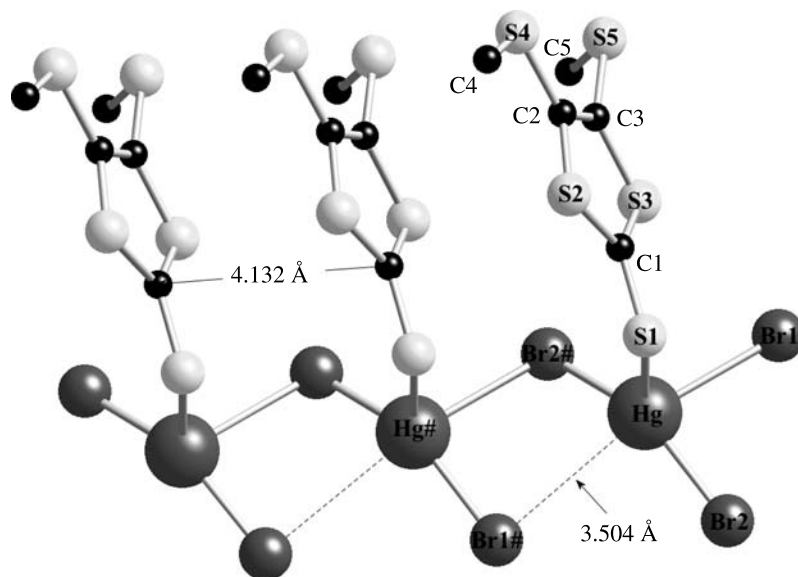


Fig. 4. View of the crystal structure of $[\text{HgBr}_2\text{L}]_n$ (**2**) along the b axis

of plane. In addition to the weak interchain $\text{Hg} \cdots \text{Cl}$ interactions mentioned above, some $\text{S} \cdots \text{S}$ contacts shorter than the sum of the corresponding *van der Waals* radii are observed in the case of **3**. Therefore, an incipient formation of a supramolecular network due to those weak interchain contacts may be taken in consideration (Fig. 5).

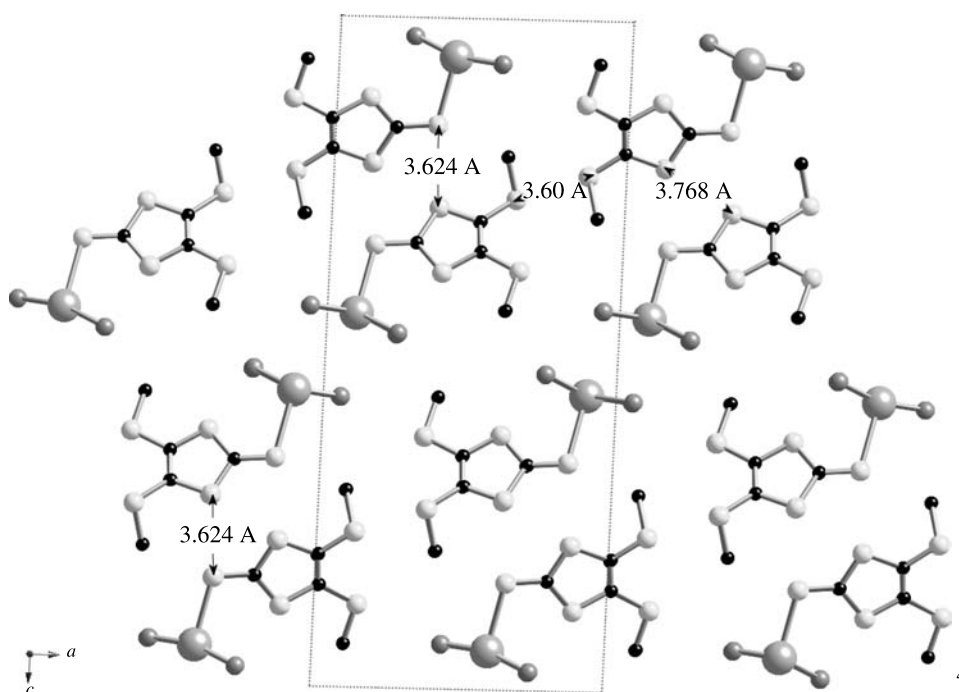


Fig. 5. Projection of the unit-cell content of **3** onto the (a, c) plane showing the inter-ribbons $\text{S} \cdots \text{S}$ interactions

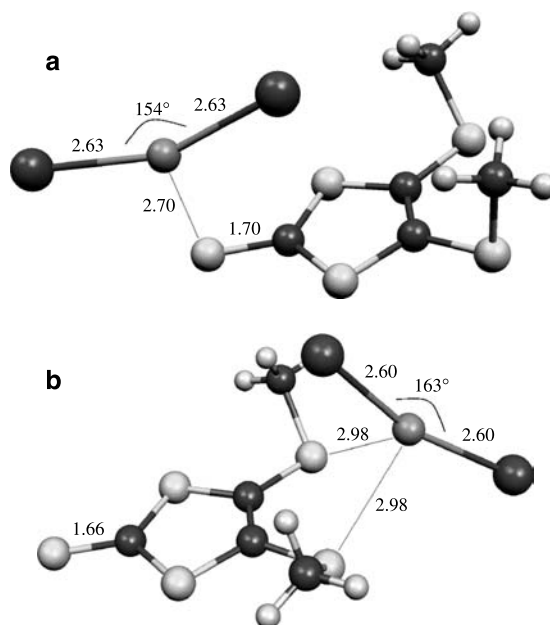


Fig. 6. The optimized geometries of the thiocarbonyl (a) and dithioether (b) adducts in the gas phase

Quantum Chemistry Calculations

The coordination mode of **L** on HgI_2 was further investigated by performing *ab initio* calculations on the two isomeric structures: the thiocarbonyl and the thioether adducts. The optimized geometries of the two adducts for the gas phase are presented in Fig. 6. In both cases, the plane determined by the three atoms in HgI_2 is a molecular symmetry plane. In the case of the thiocarbonyl adduct, the calculated Hg–S bond length is 2.70 Å, a value quite close to the experimental bond distance found in the crystal structure of **1** (2.583 Å). The corresponding computed bond length for the thioether adduct is significantly longer (2.98 Å), suggesting a weak interaction between Hg and the two chelating S atoms. This calculated value is almost identical with the Hg–S bond distance of 2.9549(10) Å found for the thioether compound $[\text{HgBr}_2\{\text{Si}(\text{CH}_2\text{SMe})_4\}]_n$ [**4c**]. An indirect indication about the importance of the charge transfer interaction between Hg and **L** is provided by the distortion of the I–Hg–I angle with respect to that of free HgI_2 (which is linear in the gas phase).

This distortion shown in Fig. 6 is more pronounced for the thiocarbonyl adduct (154°) than for the dithioether adduct (163°). Moreover, the calculated Hg–I bond distance is also somewhat longer for the thiocarbonyl adduct (2.63 Å) than for the dithioether chelate (2.60 Å). Despite these geometrical differences, we found the enthalpy difference between the two isomers to be less than 0.85 kJ mol⁻¹. This result suggests that in the crystalline state, the preference for the thiocarbonyl bonding of the $[\text{HgI}_2\text{L}]$ complex is principally due to the bridging interactions between adjacent HgI_2 groups, leading to a polymeric chain. In the hypothetical case of chelating thioether bonding, a dimeric motif should be obtained, similar to that recently found for $[\text{HgBr}_2\{(\text{PhSCH}_2)_2\text{SiPh}_2\}]$ [**4b**]. Further theoretical work to

study the solid-state structure of $[\text{HgX}_2\text{L}]_n$ and to evaluate the additional bonding contributions of π -stacking and $\text{S}\cdots\text{S}$ interactions is in progress.

Conclusion

We have shown that regardless of the nature of the halide, mercury(II) halides form upon treatment with 4,5-bis(methylthio)-1,3-dithiole-2-thione (**L**) the 1D coordination polymers $[\text{HgX}_2\text{L}]_n$. In these molecular wires, the ligand coordination occurs exclusively *via* the thiocarbonyl function. However, the coordination sphere around Hg is influenced in a subtle manner from the nature of the halide and changes from tetrahedral to distorted square pyramidal. In a forthcoming paper, we will study the conductivity of these sulfur-rich systems and evaluate the possibility to assemble heterometallic metallopolymers containing dithiolene-type ligands.

Experimental

The 4,5-bis(methylthio)-1,3-dithiole-2-thione ligand (**L**) was prepared according to Ref. [10]. Elemental analyses (C, H, S) were conducted on a Leco Elemental Analyzer CHN 900 and were found to agree favorably with the calculated values.

$[\text{Hg}(\mu\text{-Me}_2\text{dmit})\text{I}_2]_n$ (**1**, $(\text{C}_5\text{H}_6\text{HgI}_2\text{S}_5)_n$)

To a solution of 59 mg HgI_2 (0.13 mmol) in 10 cm^3 hot toluene was added a solution of 1 equiv of 4,5-bis(methylthio)-1,3-dithiole-2-thione (30 mg, 0.13 mmol) in 2 cm^3 toluene. After stirring 0.5 h at 110°C, the solution was cooled at rt and filtered. Red crystals (63 mg, 71%) in the form of fine needles suitable for an X-ray measurement were obtained after cooling the solution over night at 4°C. IR (KBr): $\bar{\nu} = 2925, 2851, 1445, 1416, 1019 \text{ cm}^{-1}$.

$[\text{Hg}(\mu\text{-Me}_2\text{dmit})\text{Br}_2]_n$ (**2**, $(\text{C}_5\text{H}_6\text{Br}_2\text{HgS}_5)_n$) and $[\text{Hg}(\mu\text{-Me}_2\text{dmit})\text{Cl}_2]_n$ (**3**, $(\text{C}_5\text{H}_6\text{Br}_2\text{HgS}_5)_n$)

These were synthesized in a similar manner as described for **1** from equimolar HgX_2 ($X = \text{Br}, \text{Cl}$) and **L** solutions. Dark-red crystals of **2** for X-ray measurement were obtained by slow evaporation of an acetonitrile solution of **2** (65% yield). IR (KBr): $\bar{\nu} = 2988, 2907, 1440, 1404, 1057 \text{ cm}^{-1}$. Red fine needles of **3** suitable for X-ray diffraction were obtained by slow evaporation of a diethoxyether solution of **3** (42% yield). IR (KBr): $\bar{\nu} = 2959, 2851, 1435, 1409, 1058 \text{ cm}^{-1}$.

Computational Method

Quantum chemistry calculations were performed with the GAUSSIAN 03 program package on a Windows XP operating PC equipped with an Intel Pentium IV 2 GHz processor with 1.5 GB of RAM. The optimized geometries and the corresponding vibrational frequencies were obtained at the MP2 level of the *ab initio* theory using the CEP-121G basis set combined with the *Stevens-Basch-Krauss* electron core potentials (ECP) [11]. The basis set was augmented with polarization functions as follows: a *d* function on S ($\zeta = 0.65$), a *d* function on I ($\zeta = 0.266$), and an *f* function on Hg ($\zeta = 0.40$).

Crystal Structure Determinations

Suitable crystals of **1** and **3** were mounted in an inert oil (perfluoropolyalkylether) and used for X-ray crystal structure determinations at 173 K. A suitable crystal of **2** was adhered on a glass fiber and used for X-ray crystal structure determination at 293 K. Data of **1–3** were collected on a Stoe IPDS diffractometer. The intensities were determined and corrected by the program INTEGRATE in IPDS (Stoe & Cie, 1999). An empirical absorption correction was employed using the FACEIT-program in IPDS (Stoe & Cie, 1999). All structures were solved applying direct and *Fourier* methods, using SHELXS-90 (*G. M. Sheldrick*, University of Göttingen, 1990) and SHELXL-97 (*G. M. Sheldrick*,

SHELXL97, University of Göttingen, 1997). For each structure, the non-hydrogen atoms were refined anisotropically. All of the H-atoms were placed in geometrically calculated positions and each was assigned a fixed isotropic displacement parameter based on a riding-model. Refinement of the structures was carried out by full-matrix least squares methods based on F_o^2 using SHELXL-97. All calculations were performed using the WinGX crystallographic software package, using the programs SHELXS-90 and SHELXL-97. The crystallographic data for each complex are given in Table 2. The figures were drawn using CrystalMaker for Mac 6.39.

Table 2. Crystal and refinement data for **1**, **2**, and **3**

Compound	1	2	3
Empirical formula	C ₅ H ₆ HgI ₂ S ₅	C ₅ H ₆ HgBr ₂ S ₅	C ₅ H ₆ HgCl ₂ S ₅
Formula weight	680.79	586.81	497.89
Temperature	173 K	293 K	173 K
Wavelength	0.71073 Å	0.71073 Å	0.71073 Å
Crystal system	monoclinic	monoclinic	monoclinic
Space group	<i>P</i> 2 ₁ / <i>n</i>	<i>C</i> 2/ <i>c</i>	<i>P</i> 2 ₁ / <i>n</i>
Unit cell dimensions	<i>a</i> = 15.575(3) Å <i>b</i> = 4.4296(9) Å <i>c</i> = 20.884(4) Å β = 100.92(3)°	<i>a</i> = 26.491(5) Å <i>b</i> = 4.1318(8) Å <i>c</i> = 25.218(5) Å β = 107.09(3)°	<i>a</i> = 11.590(2) Å <i>b</i> = 3.9882(8) Å <i>c</i> = 26.593(5) Å β = 91.42(3)°
Volume	1414.8(5) Å ³	2638.3(9) Å ³	1228.9(4) Å ³
Z	4	8	4
Density (calculated)	3.196 g/cm ³	2.955 g/cm ³	2.691 g/cm ³
Absorption coefficient	15.941 mm ⁻¹	18.473 mm ⁻¹	13.761 mm ⁻¹
<i>F</i> (000)	1208	2128	920
Crystal size	0.40 × 0.20 × 0.10 mm ³	0.20 × 0.20 × 0.10 mm ³	0.40 × 0.20 × 0.10 mm ³
Theta range for data collection	2.66 to 25°	3.16 to 25°	2.86 to 25°
Index ranges	-18 ≤ <i>h</i> ≤ 18, -5 ≤ <i>k</i> ≤ 5, -23 ≤ <i>l</i> ≤ 24	-30 ≤ <i>h</i> ≤ 30, -4 ≤ <i>k</i> ≤ 4, -29 ≤ <i>l</i> ≤ 29	-13 ≤ <i>h</i> ≤ 13, -4 ≤ <i>k</i> ≤ 4, -29 ≤ <i>l</i> ≤ 29
Reflections collected	9430	9739	9713
Independent reflections	2492 [<i>R</i> (int) = 0.0708]	2305 [<i>R</i> (int) = 0.1161]	2067 [<i>R</i> (int) = 0.1193]
Refinement method	Full-matrix least-squares on <i>F</i> ²	Full-matrix least-squares on <i>F</i> ²	Full-matrix least-squares on <i>F</i> ²
Data/restraints/parameters	2492/0/120	2305/0/121	2067/0/120
Goodness-of-fit on <i>F</i> ²	1.019	1.070	1.013
Final <i>R</i> indices [<i>I</i> > 2σ(<i>I</i>)]	<i>R</i> 1 = 0.0520, <i>wR</i> 2 = 0.1405	<i>R</i> 1 = 0.0636, <i>wR</i> 2 = 0.1787	<i>R</i> 1 = 0.0551, <i>wR</i> 2 = 0.1149
<i>R</i> indices (all data)	<i>R</i> 1 = 0.0871, <i>wR</i> 2 = 0.1603	<i>R</i> 1 = 0.0729, <i>wR</i> 2 = 0.1873	<i>R</i> 1 = 0.0964, <i>wR</i> 2 = 0.1265
Largest diff. peak and hole	1.317 and -1.314 e Å ⁻³	1.846 and -2.063 e Å ⁻³	1.352 and -2.253 e Å ⁻³

Crystallographic data for the structural analyses have been deposited with the Cambridge Crystallographic Data Center, CCDC Nos CCDC 291803, 291804, and 291805 for compounds **1**, **2**, and **3**. Copies of this information may be obtained free of charge from: The director, CCDC, Union Road, Cambridge, CB2 IEZ, UK (Fax: +44-1223-336033, e-mail: deposit@ccdc.cam.ac.uk, or www: <http://www.ccdc.cam.ac.uk>)

Acknowledgements

This work was supported by the Centre de Coopération Universitaire Franco-Bavarois.

References

- [1] For reviews see: a) Pullen A, Olk RM (1998) *Coord Chem Rev* **188**: 211; b) Kato R (2004) *Chem Rev* **104**: 5319; c) Faulmann C, Casoux P (2004) solid state properties (electronic, magnetic, optical) of dithiolene complex-based compounds. In: Stiefel E (ed) *Progress in Inorganic Chemistry*, vol 52. Wiley-Interscience, p 399
- [2] For examples see a) Munakata M, Kuroda-Sowa T, Maekawa M, Hirota A, Kitagawa S (1995) *Inorg Chem* **34**: 2705; b) Jia C, Zhang D, Liu CM, Xu W, Hu H, Zhu D (2002) *New J Chem* **26**: 490; c) Dai J, Munakata M, Bian GQ, Xu Q, Kuroda-Sowa T, Maekawa M (1998) *Polyhedron* **17**: 2267; d) Zhong JC, Misaki Y, Munakata M, Kuroda-Sowa T, Maekawa M, Suenaga Y, Konaka H (2001) *Inorg Chem* **40**: 7096; e) Dai J, Yang W, Ren ZG, Zhu QY, Jia DX (2004) *Polyhedron* **23**: 1447; f) Lu W, Yan ZM, Dai J, Zhang Y, Zhu QY, Jia DX, Guo WJ (2005) *Eur J Inorg Chem* 2339; g) Dai J, Munakata M, Kuroda-Sowa T, Suenaga Y, Wu LP, Yamamoto M (1997) *Inorg Chim Acta* **255**: 163; h) Lee HJ, Nam HJ, Noh DY (1999) *Bull Korean Chem Soc* **20**: 1368; i) Endres H (1986) *Z Naturforsch* **41b**: 1351
- [3] a) Uemura T, Kitagawa K, Horike S, Kawamura T, Kitagawa S, Mizuno M, Endo K (2005) *Chem Comm* **48**: 5968; b) James SL (2003) *Chem Soc Rev* **32**: 276; c) Batten SR, Murray KS (2003) *Coord Chem Rev* **246**: 103; d) Brammer L (2004) *Chem Soc Rev* **33**: 476
- [4] a) Peindy H, Guyon F, Knorr M, Strohmam C (2005) *Z Anorg Allg Chem* **631**: 2397; b) Knorr M, Peindy H, Guyon F, Sachdev H, Strohmam C (2004) *Z Anorg Allg Chem* **630**: 1955; c) Peindy H, Guyon F, Knorr M, Smith B, Farouq J, Islas S, Rabinovich D, Golen J, Strohmam C (2005) *Inorg Chem Comm* **8**: 479; d) Jacquot-Rousseau S, Khatyr A, Schmitt G, Knorr M, Kubicki MM, Blacque O (2005) *Inorg Chem Comm* **8**: 610; e) Peindy H, Guyon F, Jourdain I, Knorr M, Schildbach D, Strohmam C (2006) *Organometallics* **25**: 1472
- [5] a) Guyon F, Jourdain I, Knorr M, Lucas D, Monzon T, Mugnier Y, Avarvari N, Fourmigué M (2002) *Eur J Inorg Chem* 2026; b) Guyon F, Lucas D, Jourdain I, Fourmigué M, Mugnier Y, Catey H (2001) *Organometallics* **20**: 2421; c) Jourdain I, Fourmigué M, Guyon F, Amaudrut J (1999) *J Chem Soc Dalton Trans* **18**: 1834
- [6] Grdenic D (1965) *Q Rev* **19**: 303
- [7] Dai J, Wang X, Bian GQ, Zhang JS, Guo L, Munakata M (2004) *J Mol Struct* **690**: 115
- [8] Simonsen O, Varma K, Clark A, Underhill A (1990) *Acta Cryst* **C46**: 804
- [9] Nunez Gaytan ME, Bernes S, De San Miguel Guerrero ER, Bernal JP, De Gyves J (1998) *Acta Cryst* **C54**: 49
- [10] Steimecke G, Sieler HJ, Kirmse R, Hoyer E (1979) *Phosphorus Sulfur* **7**: 49
- [11] a) Sevens W, Basch H, Krauss J (1984) *J Chem Phys* **81**: 6026; b) Cundari TR, Stevens W (1993) *J Chem Phys* **98**: 5555